A Computational Method For Evaluating Astronomical Filters

by

Jim Thompson, M.Eng, P.Eng

March 2012

Table of Contents

List of Figures

List of Tables

1.0 Introduction

Over the past two and a half years I have dedicated a lot of my time to researching and reporting on the usage of astronomical filters. My research began initially dedicated to the use of filters with visual astronomy; live observing with a telescope and eyepiece. In January 2011 I made a quick transition away from observing with an eyepiece to observing with an astro-video camera, more specifically a colour Mallincam. Since then I have aimed my research at the use of filters in video astronomy, although I have tried to keep my work applicable to both methods of live observing.

In the magazine articles I have authored, I have attempted to introduce everyone to astronomical filters, from simple colour filters for planetary work through to hi-tech light pollution filters for deep-sky. Based on price alone, I imagine that the amateur astronomer is most interested in choosing the right light pollution (LP) filter. A hundred dollars (or more) is a lot to invest in a piece of glass that may not actually do anything. I have performed my own tests on LP filters, both with an eyepiece and an astro-video camera. My tests have been limited to only a couple of different filter types and brands. The sheer numbers of filters on the market make it not affordable for me to compare them all side-by-side using observations. In addition, there are so many filters to compare, it would be impossible to do so under exactly the same conditions. It was this problem that inspired me to develop a computational method for comparing filters.

The method I have developed involves the manipulation of large tables of data, which a computer can do very well. One of the results of my research into filters has been the creation of a filter spectral response database. Some response curves are from technical papers, many are from websites, some are from filter packaging that astronomy supply store owners have been nice enough to scan for me, and some I have even measured myself. All totaled I have spectral response curves for over 100 interference type filters, plus approximately another 50 colour filters. My method in principle consists of multiplying the spectral response of each filter times the emission spectrum of a typical deep-sky object (DSO), and then passing it through the spectral response of the desired detector (human eye or CCD). The resulting net perceived emission from the DSO is then compared to the background to determine how "visible" the object is. A calculation with no filter is used as the baseline for comparison. In the remainder of this paper I will explain in detail how this calculation is done.

2.0 Inputs & Assumptions

Filter Data

The first thing I did was format my filter data so that it was amenable to doing calculations on it. The filter data I have compiled comes from numerous sources. Almost all of the spectral response data I have came to me in the form of an image file or PDF containing the filter's spectral response curve. A great amount of time was spent converting these images into tables of filter response versus wavelength data. My procedure consisted of the following:

1. Import image of response curve into suitable vector drawing software such as Corel Draw.

2. Trace over the curve and axis of the plot using a spline and straight lines respectively, then export the spline/lines as a .DXF file.

3. Import the .DXF file into a design/drafting software. Scale the imported spline & lines into the correct units; 0 to 100% in the vertical axis, and nanometers on the horizontal axis. Move the axis to the correct absolute location in space based on the corrected units.

4. Create points along the spline at even intervals, and export the points only to a .SAT file.

5. Open the .SAT file in a simple text editor and delete all lines except those with the "point" descriptor. Save the resulting file as a .TXT.

6. Import the .TXT file into your spreadsheet software, parsing assuming a space delimited file. Manipulate the imported table of data as required.

I further parsed the data from all 14 of my deep-sky filter categories plus the colour filter data (including IR high-pass filters) so that it was continuous from 200nm to 1200nm in 5nm steps. I chose this large wavelength range in order to handle the wide spectral response of a typical CCD. In cases where I was missing data in the UV or IR bands, I filled it in with a best guess: zeros in the UV, and an average of known filter responses in the IR. The result was a large spreadsheet table, ready to multiply against something.

Category	Prerequisite
H-alpha Group A	H-alpha pass band is >10nm wide
H-alpha Group B	H-alpha pass band is <10nm wide
H-beta Group A	Pass H-beta wavelength with >90% transmission
H-beta Group B	Pass H-beta wavelength with <90% transmission
O-III Group A	Allow both doubly ionized Oxygen wavelengths to pass
O-III Group B	Allow only one doubly ionized Oxygen wavelength to pass
Narrow Band	H-beta + O-III pass band is <35nm wide
Medium Band	H-beta + O-III pass band is >35 but <50nm wide
Wide Band	H-beta + O-III pass band is >50 but <70nm wide
Extra Wide Band	H-beta + O-III pass band is >70nm wide
Multi Band	More than two major pass bands in the visible range
IR Cut	Blocks wavelengths above 700nm
Special A	Filters esp. designed for planets or other special object viewing
Special B	Special filters for contrast enhancement based on Neodymium infused glass

Table 1 Deep-Sky Filter Categories

Targets

When selecting a target DSO, I anticipated differences in filter performance depending on whether the DSO was a bright O-III rich nebula, a dim H-alpha nebula, or a galaxy. As a result I chose a typical representative from each group: M27 Dumbbell Nebula (bright nebula), NGC7000 North American Nebula (dim nebula), and M51 Whirlpool Galaxy (galaxy). Finding emission spectra for these types of objects was relatively easy. There is a lot of research ongoing in this area, making data readily available on the internet. The spectrum for M27 I selected is a direct measurement of the actual object, but the other two are amalgamations of spectral responses from a number of sample objects. For my purposes only a representative emission spectra was required, so using an amalgamation was adequate.

Object	Visual Magnitude	Relative Brightness	Angular Dimensions (arc min or arc sec)	Projected Area (sq arc sec)
Star - α Lyrae "Vega"	+0.03	1	0.006"	*
Planetary Nebula - M27 "Dumbbell"	+7.5	0.001	8' x 5.6'	63, 900
Emission Nebula – NGC7000 "North American"	+4	0.025	120' x 100'	43,200,000
Galaxy – M51 "Whirlpool"	+8.4	0.00044	11' x 7'	92,300

***** Minimum resolvable airy disk diameter when viewing Vega with assumed telescope is 1.54", resulting in projected area of 1.87 sq arc sec.

Table 2 Selected DSO Assumptions

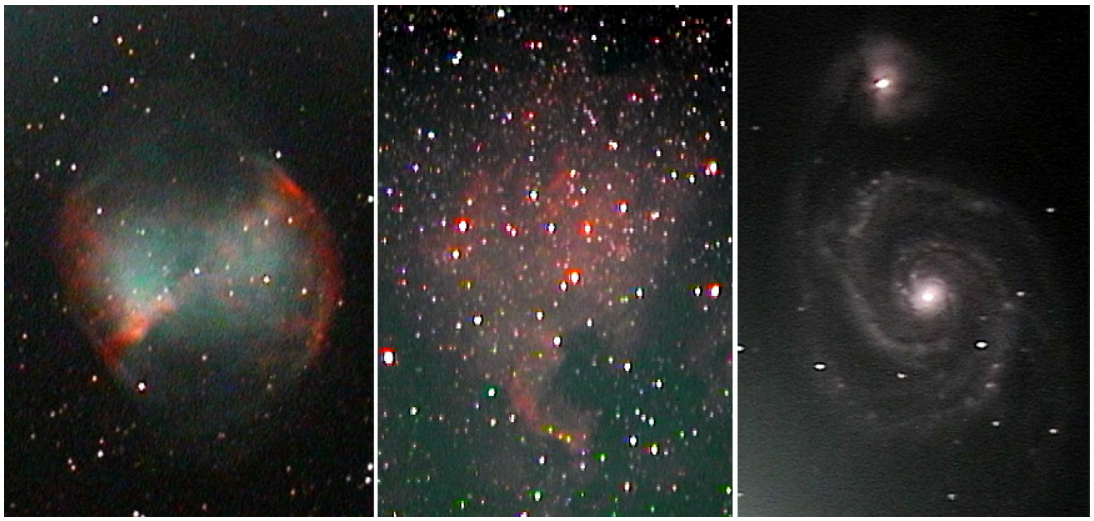

Figure 1 Selected DSO Targets: M27, NGC7000, & M51

Also of interest was the emission spectra of the star Vega (α Lyrae), as will be explained later. The emission spectra was all parsed similarly to the filter data; 200 to 1200 nm in 5 nm steps. The data was also normalized and tabulated, ready for use along with the filter data.

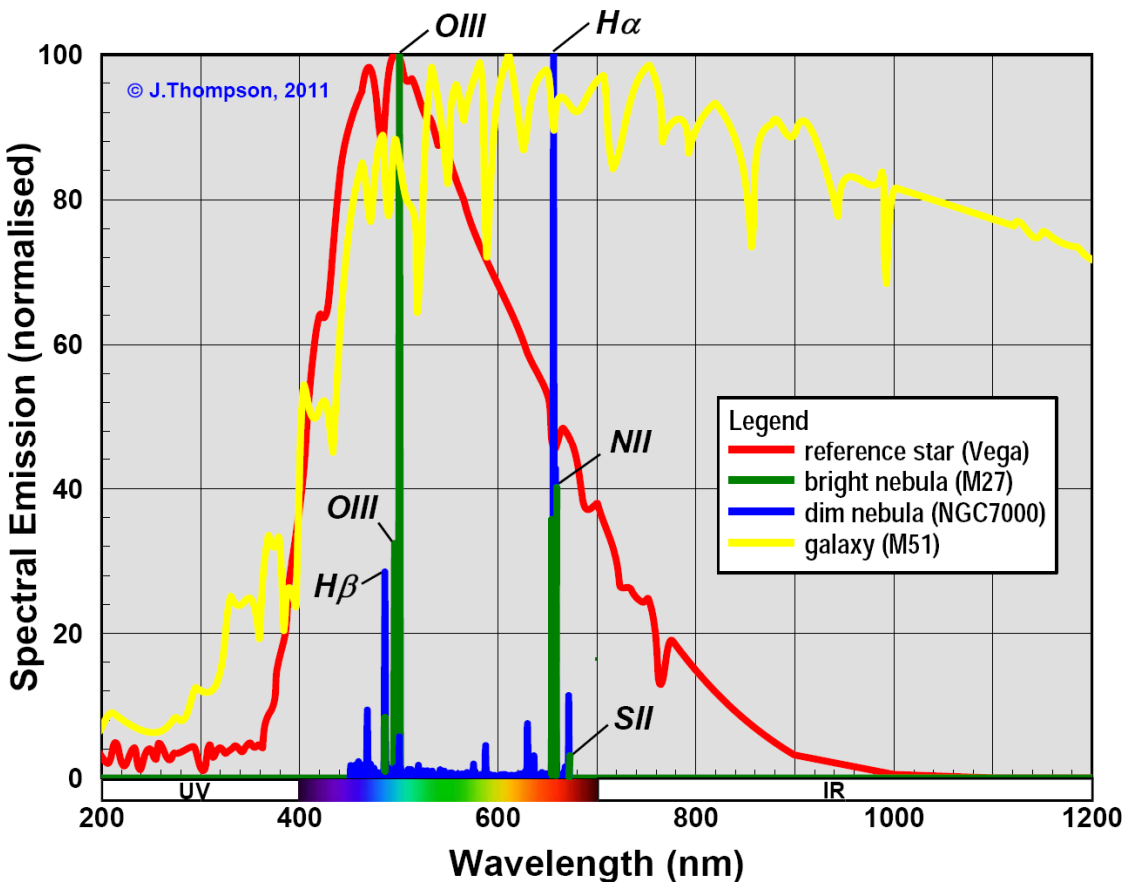

Figure 2 Normalized Emission Spectra for the Selected DSO's

Detector & Optics

Next I selected my detectors: the dark adapted (scotopic) human eye, and the Sony ICX418AKL colour CCD. This particular CCD was selected since it is the sensor that is in my astro-video camera, a Mallincam Xtreme. The CCD has a significantly higher sensitivity in the red and near infrared parts of the spectrum compared to the eye, so I was very interested to see how the two compared to each other. Figure 3 includes spectral responses for two other CCD's used in Mallincam brand astro-video cameras. Again, this data was all originally in raster image form and had to be converted to vector using the procedure described above.

Once I began my rough calculations I quickly determined that I also had to choose a reference telescope configuration. I chose a configuration relevant to my own observing: an 8" f/10 Schmidt-Cassegrain with eyepiece/camera effective focal length of 8mm. This gives about 250x power, and a field of view of approximately 12 arc minutes.

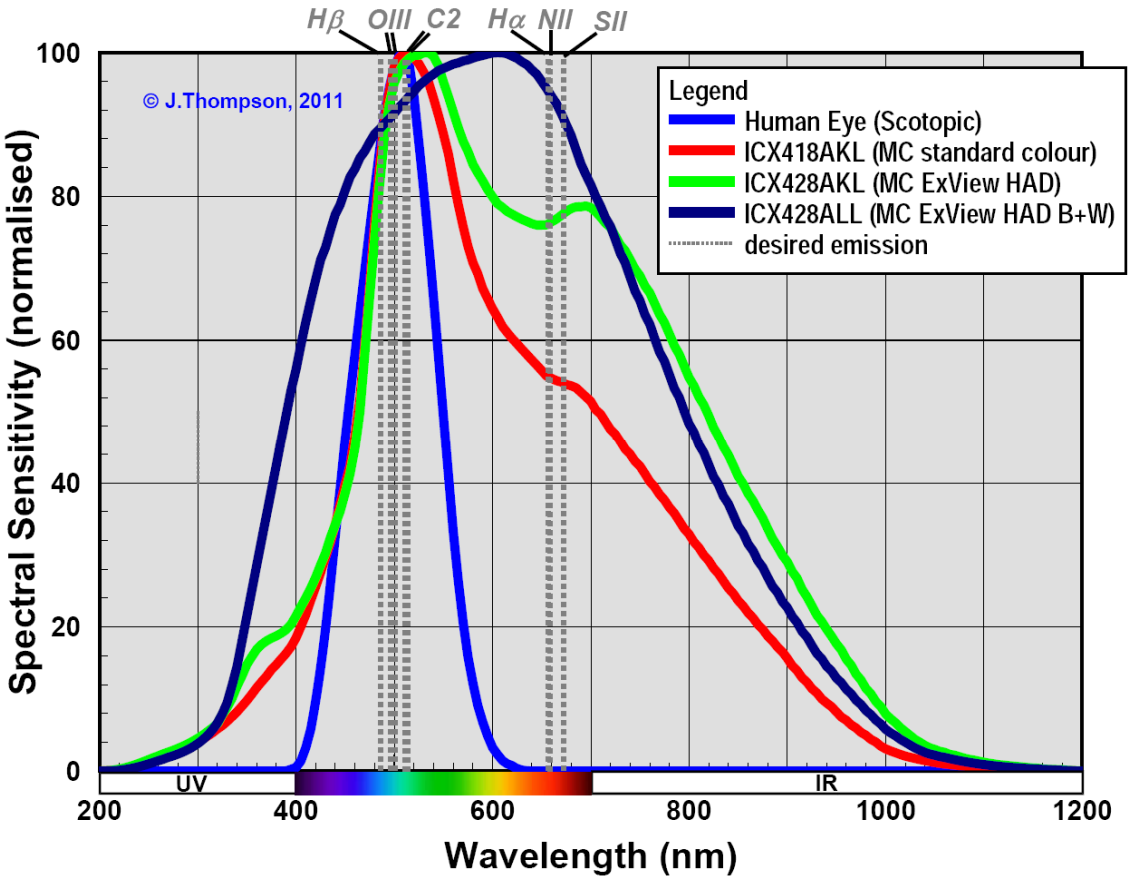

Figure 3 Detector Spectral Sensitivity Comparison

Sky Emission

The last input to my calculation was representative spectral data for a typical nighttime sky. Of particular interest to me was a sky that represents on average the level of light pollution that I observe under from my backyard in Ottawa, Canada. Also of interest were a "dark" sky and a moonlit sky in the city, representing the best and worst sky conditions I would ever expect to observe under. Establishing emission spectra for these cases was difficult, but I managed to do it by separating the sky emission into independent components of pollution. I decided to base my sky emissions on the notion of "limiting visual magnitude". Under natural dark skies, the dimmest star you can see with the unaided eye is around MAG +7. Any glow seen in the sky under these conditions is due to natural phenomenon like ionized Oxygen or Sodium in the upper atmosphere. Where I live the average limiting magnitude is about MAG +3.5. The sky glow is due to not only the natural contributors, but also the unwanted contribution of man-made outdoor lighting. On evenings when the Moon is full or nearly so my limiting magnitude is more like +2. In this case the sky glow is a sum of natural sky, man-made LP, and the Moon.

Figure 4 My Meade 8" SCT on Orion Atlas EQ/G Mount with Mallincam Xtreme

Finding independent spectra for each of these three contributors (skyglow, light pollution, & Moon) was very difficult. In the end I only found a complete emission spectrum for the Moon. I constructed the other two on my own based on segments of spectra that I was able to find. The resulting spectra may not be completely accurate, but I believe they are at least representative.

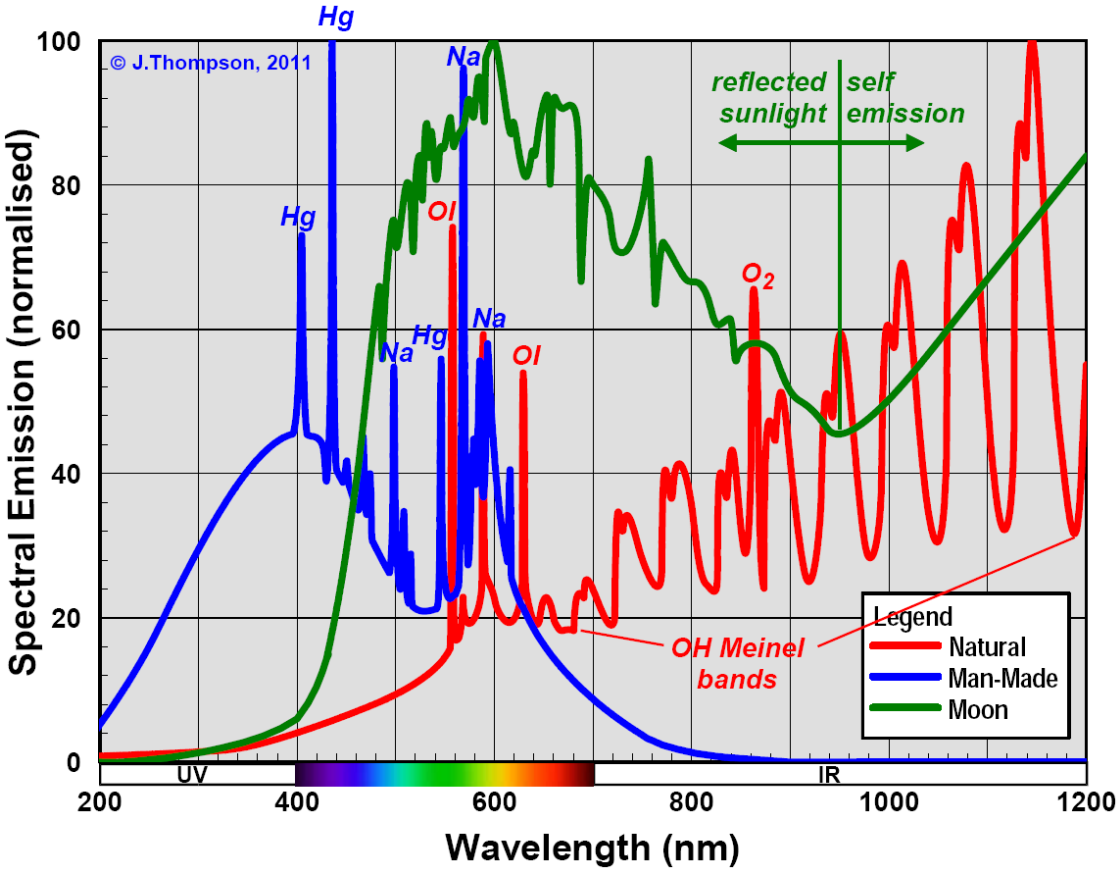

Figure 5 Emission Spectra for Light Pollution Contributors

3.0 Dimensionalizing Emission Data

All the spectral emission data that I collected was originally found in a broad range of units. In the process of parsing and tabularizing that data, I normalized it all in terms of a percentage of full scale. To be able to combine and compare this data I had to convert it all into a common scalar unit. The key to this conversion was the star Vega. The star visual magnitude system is referenced from Vega which many years ago was set to Mv 0.0. It is actually not quite magnitude zero today, but it is close enough for my needs. The visual magnitude system is a logarithmic expression of apparent brightness relative to Vega:

$$Mx = -2.5\log_{10}(Fx/Fx^{0})$$

By multiplying the normalized spectral emission data for Vega times the spectral response of the human eye, and integrating across the visual range of wavelengths (400 to 700nm), the resulting number represents how many "units" of light the human eye receives from this target. To express this number in terms of luminance (brightness per unit area), I used an estimate of the projected area of Vega, taking into account the minimum resolution of my selected telescope setup. With a value of luminance for Vega established, I was able to use it as a unit of measure against which all the other emission spectra were compared. Each emission spectra was multiplied by the human eye spectral response, and the result integrated across the visual band. I then divided by the estimated projected area of each object to get luminance. I divided this number by the result for Vega to get a value for relative brightness. This calculated relative brightness was then compared to what is normally accepted for each object: +7, +3.5, and +2 for the three backgrounds; and +7.5, +4, and +8.4 for M27, NGC7000, and M51 respectively. I had to apply a correction to the accepted visual magnitudes to account for the fact that I was observing these objects through a telescope. The correction is based on the aperture, magnification, and assumed transmissivity of the optics:

$$Mtel = Meye -2 + 2.5\log_{10}(D*P*\tau)$$

, where D = aperture (203mm), P = magnification power (250x), and τ = optics transmissivity (~0.9). The factor by which the two relative brightness numbers were off gave me the factor by which I needed to scale my emission spectra so that they were in the same units as Vega and thus each other. Figure 6 presents how the resulting scaled emission spectra look relative to each other. Note that the different sky emissions shown are sums of the emission spectra for each of the relevant individual components; skyglow, light pollution, and Moon. The three DSO spectra were scaled up by an additional factor of 3.0, as will be explained later.

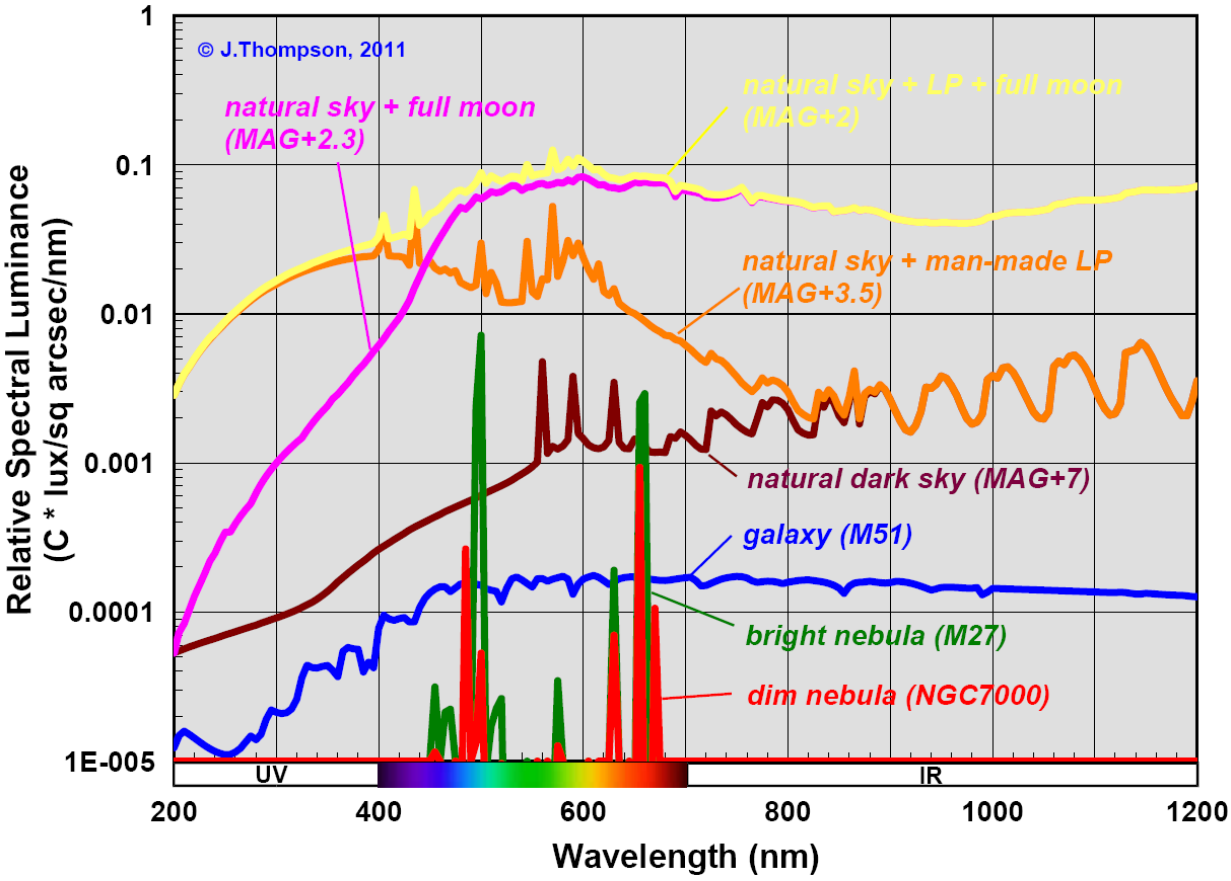

Figure 6 LP & DSO Emission Spectra in Absolute Scalar Units

4.0 Visibility – Human Eye

In the few years leading up to my starting the development of this analytical method, I have observed all three of the selected DSO's from both my home in Ottawa and a dark site up at our family cottage. Observation was done using both an eyepiece and an astro-video camera, using the telescope configuration that has been selected for my calculation. I have also used a couple of different light pollution filters during that time. Based on these observations, I have a pretty good idea of how visible the selected DSO's are under a range of conditions. I used this information to confirm that my analysis method was on track.

The objective of the calculation is to determine how much more visible the DSO is using a particular filter. The measure of visibility I am using is how different in luminance the DSO is compared to the surrounding background. The human visual system, including eye and brain, is complex. To keep things simple I have used a rule of thumb that I remember from a 1990's science show called "Connections". The rule of thumb is that the human visual system can detect a change in brightness of 1 in 50. I used this as my threshold for detection: an object is visible relative to the background if it is brighter than the background by 2% or more. In my calculation I express this as a Signal-to-Noise Ratio (SNR):

$$SNR = (Luminance_{DSO} + Luminance_{sky}) / Luminance_{sky}$$

Thus, an object is considered to be visible for an SNR of 1.02 or more. Also, the amount by which the SNR increases when using a light pollution filter over no filter is a direct measure of how affective the LP filters is.

The calculation up to this point has made many assumptions regarding emission spectra, DSO sizes and magnitudes, etc. It was important at this stage to perform a sanity check to confirm that the SNR values predicted by my method were consistent with actual observation. I used my method to calculate the SNR with no filter and with my usual LP filter for each object. I found that my prediction of visibility was too low. Multiplying the emission spectra of each of the DSO's by an additional factor of 3.0 seemed to put the predicted SNR at a level that was consistent with my observing experience. Note that the emission spectra in Figure 6 include this extra factor of 3. After this final tweak I selected a short list of filter representatives from each filter category, and passed them through the calculation.

- Multi Band: IDAS LPS-P2
- Extra Wide Band: DGM GCE
- Wide Band: Lumicon Deepsky
- Medium Band: Astronomik UHC
- Narrow Band: Meade Narrowband
- O-III: Astronomik O-III
- H-beta: Astronomik H-beta
- Special: Canadian Telescope Moon&Sky Glow

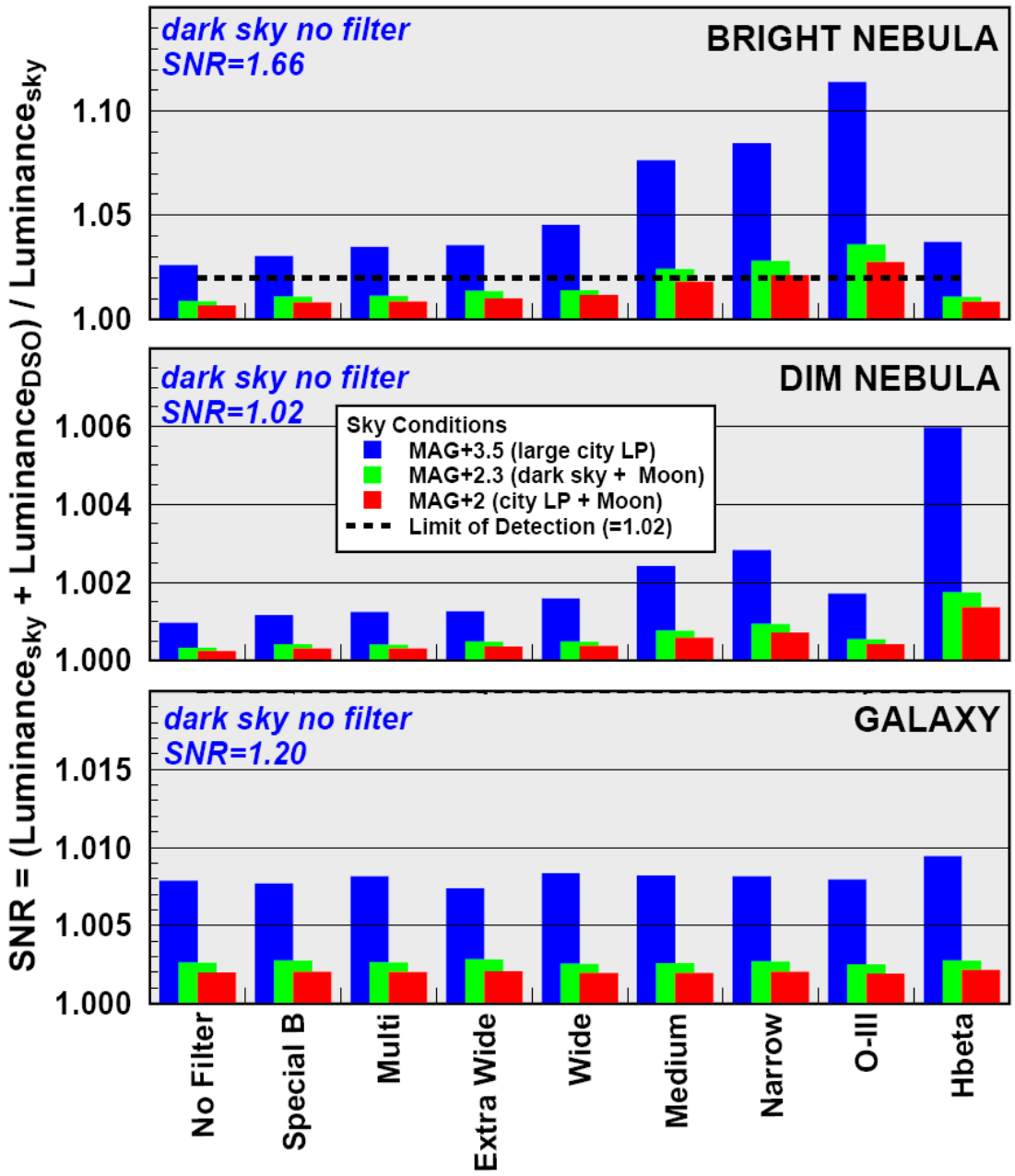

Figure 7 ***Filter Visual Performance By Category***

Based on my predictions, the bright nebula is just barely visible with light pollution and no filter when there is no Moon, but is not visible at all when the Moon is up. Adding a LP filter greatly increases the SNR, making the object much more visible even on moonlit nights. As the narrowness of the LP filter increases so does the SNR, with the O-III filter resulting in the highest contrast view. These predictions are completely consistent with my observing experience. For the dim nebula, my predictions say that I can not see this object when under

light polluted skies even with filters, and can just barely see it when under dark skies. This is also true based on my observing experience. If I were to use a faster f/ratio or larger aperture, then the H-beta filter looks like it would give the best contrast view. Finally for the galaxy, under dark skies the object is predicted to be easily visible, but when under light polluted skies it is not possible to see it, with or without a filter using my telescope setup. These two predictions are also true based on my experience.

The consistency of my predictions with my actual observations was very comforting as it confirmed that my methodology is sound. It was now time to run all the deep-sky filters in my database through the same calculation. I plotted the predicted SNR for each filter for each DSO and sky type versus the filters' luminous transmissivity (%LT). My use of the term %LT is defined as: the wavelength averaged transmissivity of a filter, weighted by the spectral response of the detector, which in this case is the dark adapted (scotopic) human eye. It is a single number that quantifies how "dark" the filter is when observing with it using our eyes at night.

When I plotted the predicted SNR values in this way, I found that all the deep-sky filters seem to follow a well defined distribution. Some outliers were observed, but most filters fit along the trends shown in Figure 8. The original SNR versus %LT plots can be found in Appendix A. This was an interesting finding since it means that choosing the best filter for your telescope setup becomes as simple as finding the lowest %LT your telescope can support based on your aperture, and picking one of the filters that sits at that location on the SNR curve. I established a recommended minimum %LT versus telescope aperture relationship during my earlier filter research, the result of which is shown in Figure 9. The curves in Figure 8 also determine the best you can hope to achieve with a filter depending on the DSO and seeing conditions. The curves can also be used to separate good filters from bad ones; good ones should be on or above the curve, bad ones are below the curve. This comparison of each filter to the standard performance curve is discussed further in a later section.

I ran all the colour filters through the same analysis, and found that they really are not effective as LP filters. On bright nebulae, a small improvement in SNR was achieved by using a green or yellow filter, but the resulting SNR is about half that of a proper LP filter of the same %LT. On dim nebulae colour filters did nothing except make the view dimmer. On galaxies green and yellow filters gave a slightly better SNR than LP filters of the same %LT, but similar to LP filters the improvement in SNR over no filter was very small; not enough to raise the SNR above the level of detection for my assumed telescope configuration. I did not generate a simplified SNR plot like Figure 8 for colour filters, but the original SNR vs. %LT plots can be found in Appendix B. I chose to include colour filters in my analysis because they are absorption type filters, which are not sensitive to the angle of the light through the filter. In applications where a very wide field of view is desired, interference type filters do not perform well. If a colour filter can be found that gives a comparable improvement in SNR to an interference filter, the colour filter would be the preferred choice when using a wide FOV instrument such as a pair of binoculars or wide angle DSLR lens.

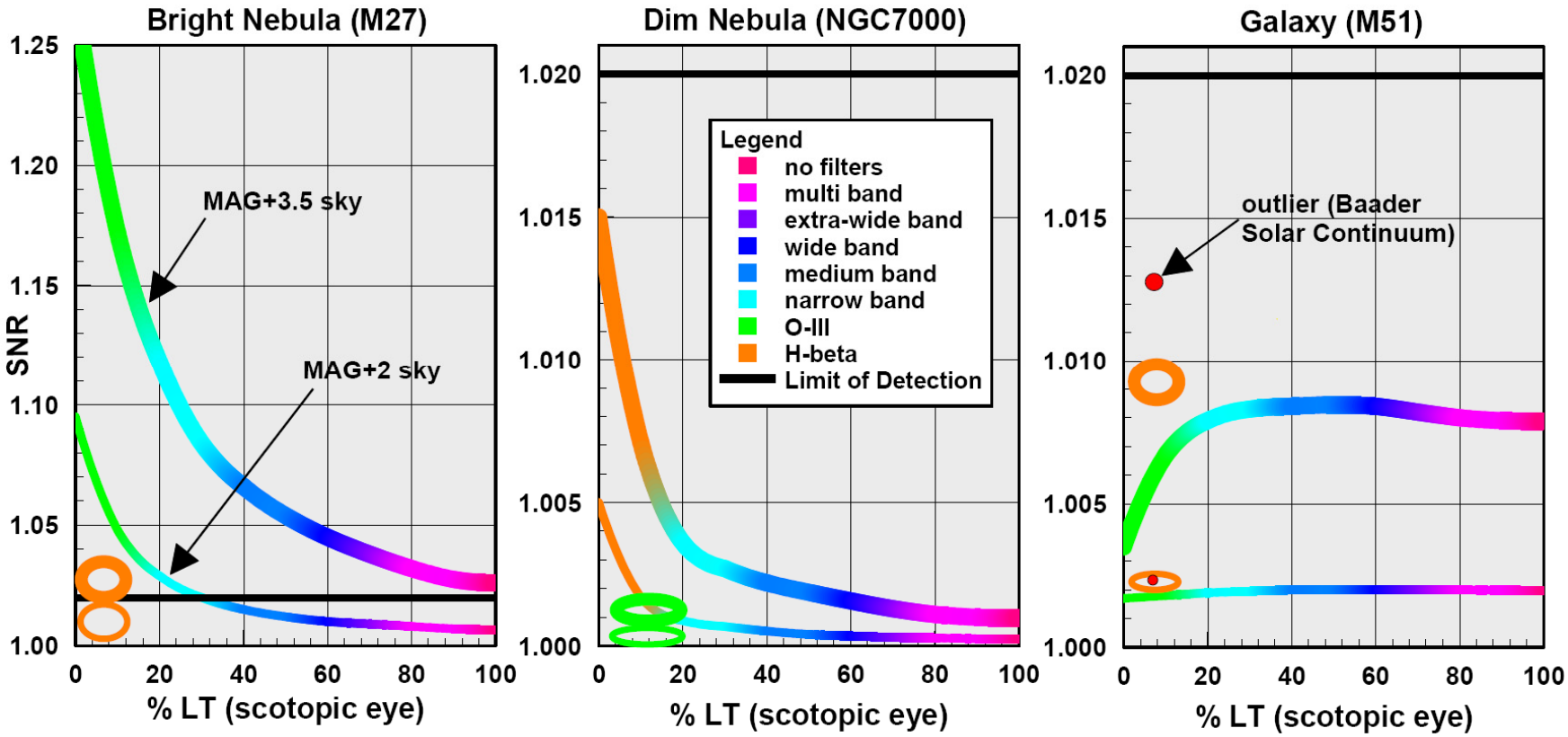

Figure 8 ***All Deep-Sky Filters - Simplified Visual Performance Comparison***

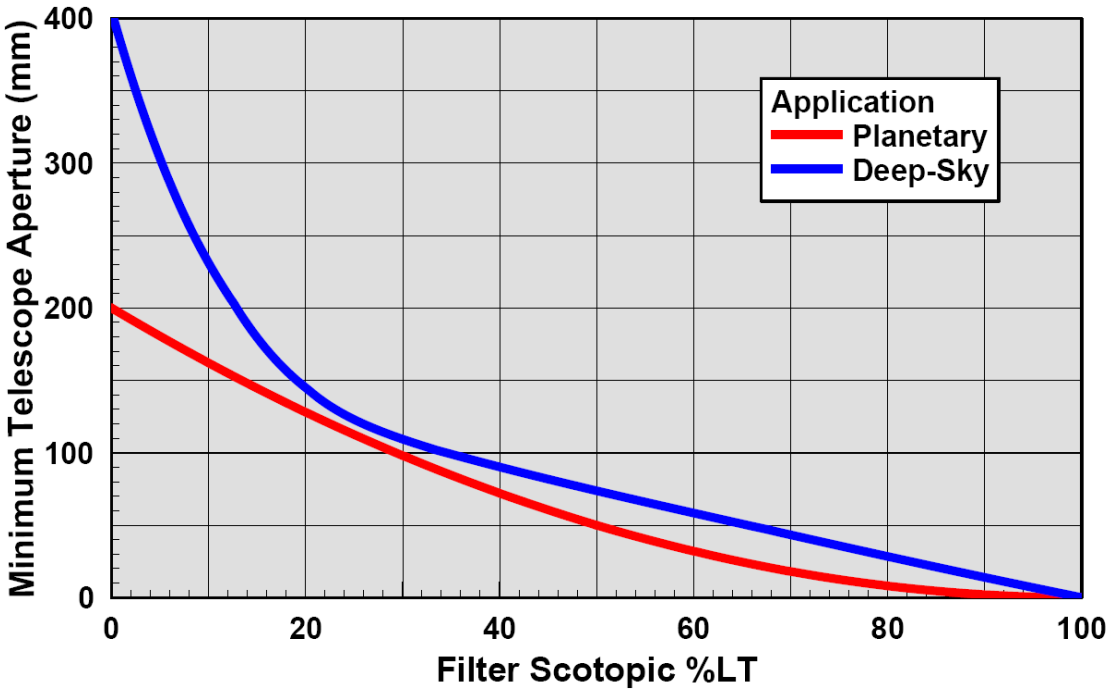

Figure 9 Recommended Minimum %LT vs. Aperture

5.0 Visibility – Mallincam

Video astronomy is a combination of live observing and imaging, and as a result it is able to take advantage of the best aspects of both fields, including the use of filters. No longer limited to viewing objects in the narrow cyan-green band that our eyes can see at night, video astronomy opens the door to using filters normally used for CCD imaging. The most notable changes over eyepiece observing is being able to see hydrogen alpha emissions from nebulae, and being able to see near-infrared emissions from galaxies. Unfortunately, astro-video cameras are also more sensitive to the main wavelengths for light pollution as well. Without using filters, an astro-video camera is able to view dim objects that would normally not be possible from inside a city. By effectively applying the right LP filter however, the views that can be achieved are simply stunning.

Being now able to use filters meant originally for imaging adds to the problem of choosing the right filter. I had to add four new filter categories in order to capture these new additions: H-alpha Group A & B, IR Cut, and IR Pass. The first three new categories are all interference type filters like the other LP filters, but the IR Pass is an absorption type; essentially a colour filter. I have not included extremely narrowband filters in my list such as NII and SII filters since the length of the integration time required to use them makes them not practical for live observing. To compare the performance of filters when used on an astro-video camera I have used the same methodology as I used for visual observing (see Section 4.0). I used the same telescope setup, same background light pollution cases, and same three DSOs. The detector selected for the analysis was the Sony ICX418AKL, the same CCD used in the standard Mallincam Xtreme. The only difference in my analysis was the unit of measure used to evaluate each filter's performance. SNR is not a good measure of performance since the video processing circuitry in the camera is able to adjust the contrast and brightness (and thus SNR) on-the-fly. Instead I chose to use the max predicted difference in RGB level between the DSO and the background. Assuming an 8-bit per colour Red/Green/Blue colour system, the maximum contrast in a video image is achieved when the DSO is at the saturation limit (RGB=255) and the background is black (RGB=0). Using the same 2% rule from before, the minimum ΔRGB level for detection of the DSO is 5. Figure 10 illustrates the appearance of a DSO on a computer monitor at varying ΔRGB levels. The predicted ΔRGB level is calculated using the following equation:

$$\Delta RGB = 255 * [1 - (Luminance_{sky}/(Luminance_{sky} + Luminance_{DSO}))] * C$$

The constant 'C' was used to calibrate my predicted ΔRGB against what I have measured in the past using my Mallincam. A value of 5.0 has been used.

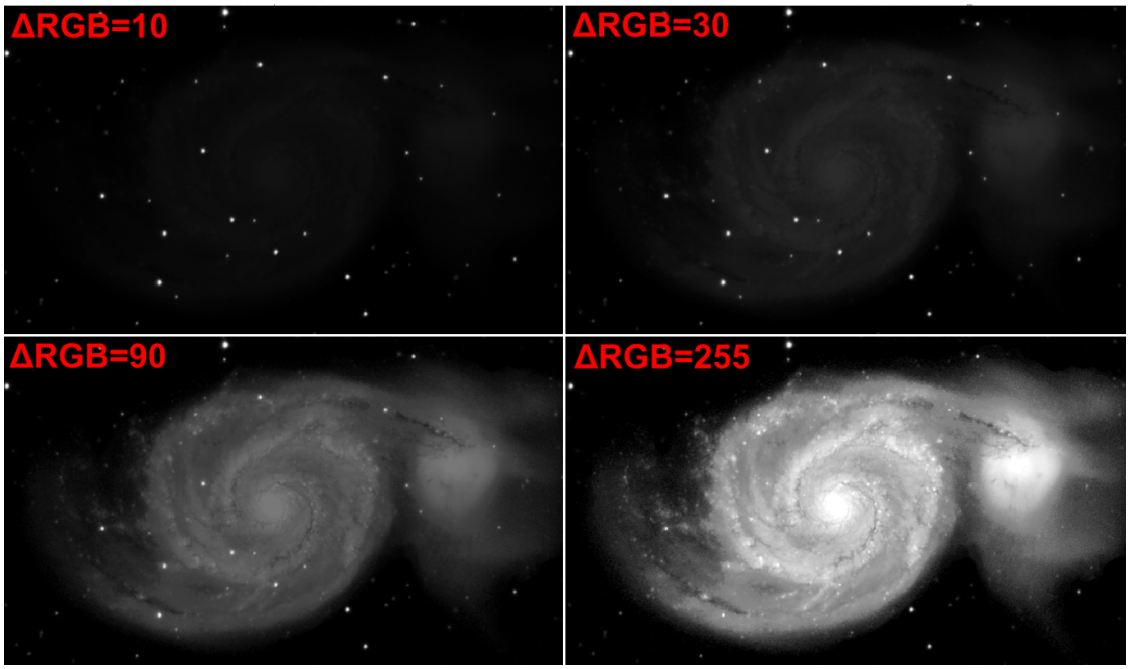

Figure 10 Visual Comparison of Different ΔRGB Levels

As with the visual analysis, I began with one representative from each of my filter categories (see Section 4.0 above). I did not include IR Cut filters as a separate category, but instead evaluated all the other filters with and without an idealized IR Cut; a filter with 100% transmission between 400 and 700nm, and 0% transmission everywhere else. I plotted the predicted ΔRGB values for a MAG +3.5 (LP), +2.3 (Moon), and +2 (LP + Moon) sky, with and without filters (see Figure 11). The plot shows the "without IR cut" performance as columns, and the "with IR cut" performance as horizontal bars of the same colour.

On bright nebulae, light pollution filters were found to be very effective at increasing ΔRGB in the image when there was no Moon out. When the Moon is out, the effectiveness of the filters was greatly reduced. This is consistent with what I have observed using my MC. Medium and Narrow band filters perform reasonably well, with the OIII filter being slightly better again. The Halpha filter provided the best level of ΔRGB, being almost equivalent to the no-filter case under dark skies. In all cases, adding the IR Cut filter to the LP filter improved the ΔRGB slightly, with the biggest improvement showing up on Medium Band, Narrow Band, OIII, and Hbeta filters.

When applied to dim nebulae, LP filters help somewhat, but not enough to bring the ΔRGB level significantly above the detection limit for my telescope setup. The exception is the Halpha filter, which was predicted to increase the ΔRGB to a level several times more than what would be achievable with no filter under dark skies. Even with the Moon up, the Halpha filter increased the ΔRGB level above the detection limit. Applying an IR Cut filter did improve filter performance slightly, as was observed for bright nebulae.

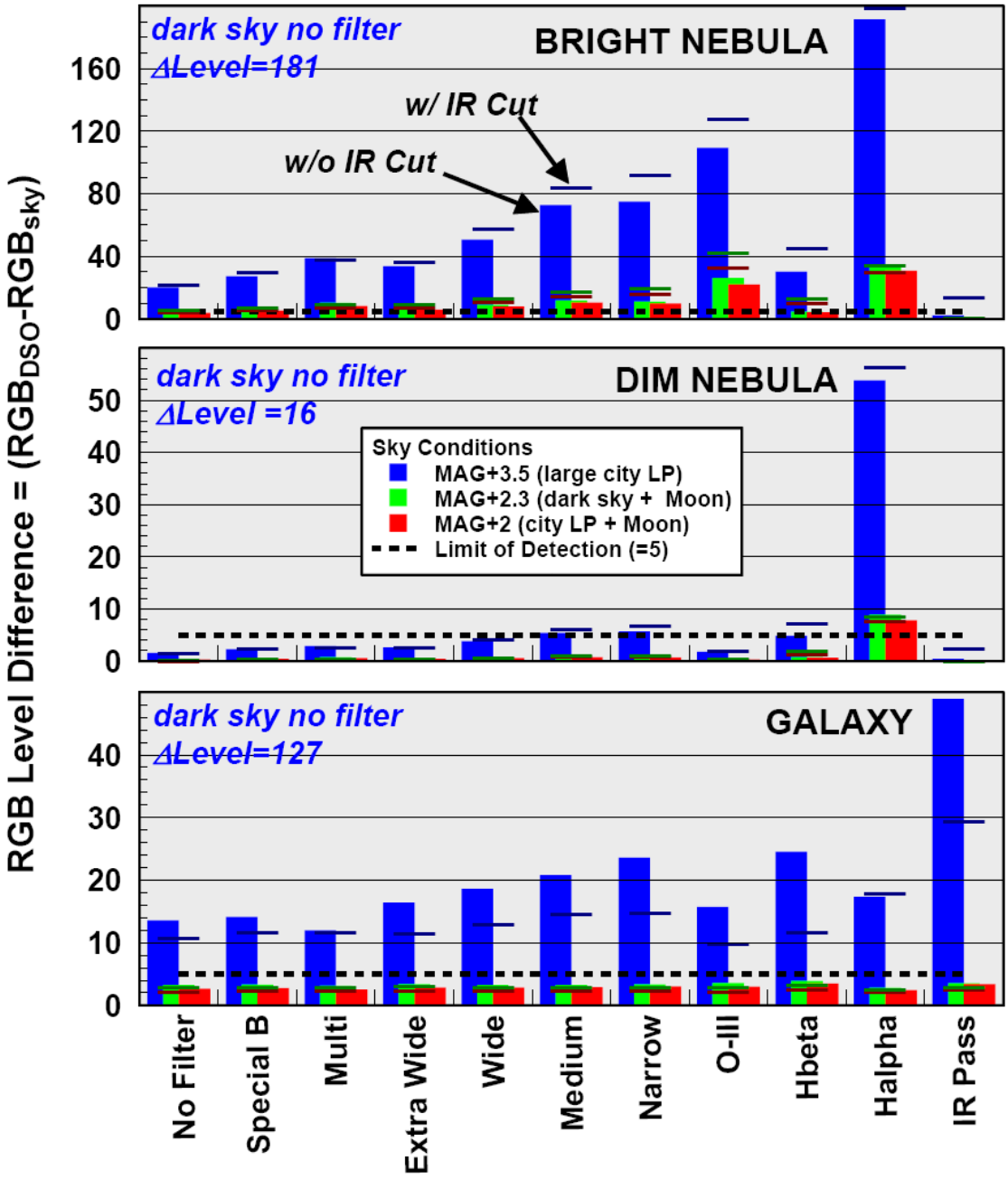

Figure 11 Filter Video Performance By Category

When LP filters were used on the galaxy, there was a small improvement in ΔRGB. The Medium Band, Narrow Band, and Hbeta filters provided the best improvement out of the LP filters tried. More interesting was the large improvement in ΔRGB realized by using the IR Pass filter. This filter was able to produce ΔRGB levels twice that predicted for the LP filters. For all filters, adding an IR Cut resulted in a significant drop in ΔRGB, the opposite of what was found when viewing nebulae. I have confirmed by test all of these observations on galaxies, and for

the most part found them to be true (test reports are available upon request that summarize these observations). The only exception is that my analysis predicts that even with LP filters, galaxies are not detectable with my telescope setup when the Moon is up. In practice I have found that galaxies are detectable when the Moon is out, albeit at a much decreased ΔRGB, and their view is improved with the use of an LP filter. This observation varies depending on the surface brightness of the particular galaxy, ie. low surface brightness galaxies are indeed not visible with my setup when the Moon is out. The consistency between my predictions and actual observations gave me confidence to proceed with analyzing the rest of the filters in my library.

Similar to what was done in Section 4.0, I plotted the predicted ΔRGB for each filter versus its Luminous Transmissivity (%LT), in this case %LT being calculated using the ICX418AKL as the detector. Doing so revealed some very definite trends in filter performance. Figure 12 shows a simplified version of the results, identifying the general trend in performance for the different filter categories. The full plots can be found in Appendix C. I found there to be a large amount of scatter in the results. The scatter is due to the fact that most LP filters, being designed for visual use, do not all pass Halpha and Near Infrared to the same extent. Some filters are clearly superior due to them including good Halpha and NIR responses in their design. The plots in Figure 12 also show the magnitude and direction of shift in filter performance when an IR cut filter is added; up and left on nebulae, down and left on galaxies.

On bright nebulae, Halpha and O-III filters appear to provide by far the best contrast. With no Moon, narrowband Halpha filters edge out O-III slightly, to the point of getting saturation in the nebula image when the integration is maximized. When the Moon is out, O-III filters seem to edge out Halpha. Narrow and Medium Band LP filters also provide a good improvement in image contrast at a much decreased integration time over Halpha and O-III filters. Dim nebulae benefit from LP filters much like bright nebulae do. The performance of O-III filters is reduced to the point of being useless on this type of target, but Hbeta filters step up to fill the roll. Again Halpha filters are the best performers for contrast over Hbeta and Narrow Band filters, at the cost of longer integration times. When the Moon is up, it would appear that Halpha filters are the best bet on dim nebulae. The performance of LP filters on galaxies was the most scattered plot of them all. The response of LP filters in the NIR band seems to play a large part in how well each filter performs. Of the conventional multiband LP filters, Medium Band filters seem to perform the best. I was surprised at how well Hbeta filters were predicted to perform. This result prompted me to include an Hbeta filter in a recent test with my MC, the result being my prediction seems to be true, but to an extent less in practice than predicted by my analysis. Figure 13 shows the results of a recent test I performed where I observed M33 with a number of different LP filters using my Mallincam. I calculated the measured ΔRGB from the recorded video frames, and plotted them against the predicted values for the same filters. The correlation is very good between measured and predicted values, with variations likely being due to differences in the way I set the video brightness from filter to filter. More detail about this test can be found in my test report titled: "Managing IR In Video Astronomy – Part 4".

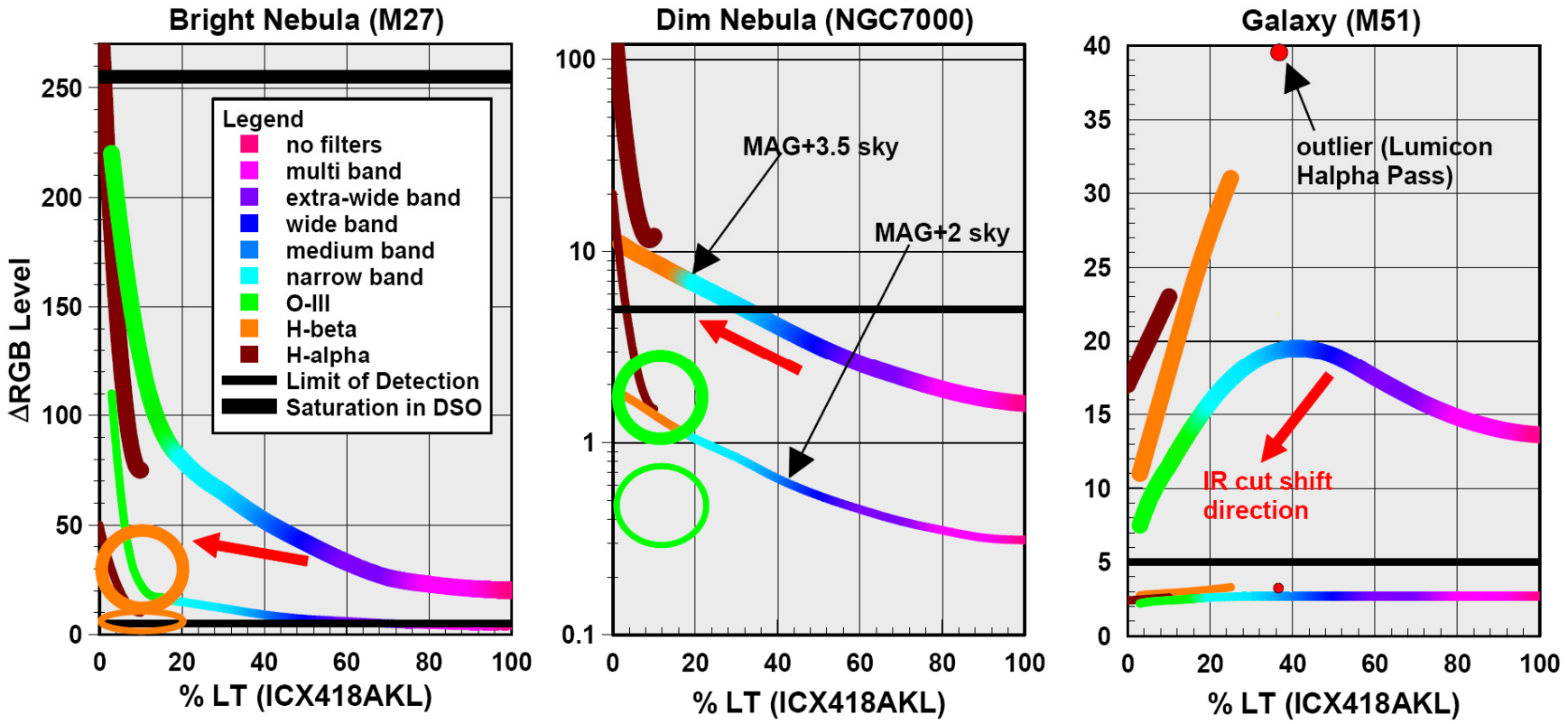

Figure 12 All Deep-Sky Filters - Simplified Video Performance Comparison

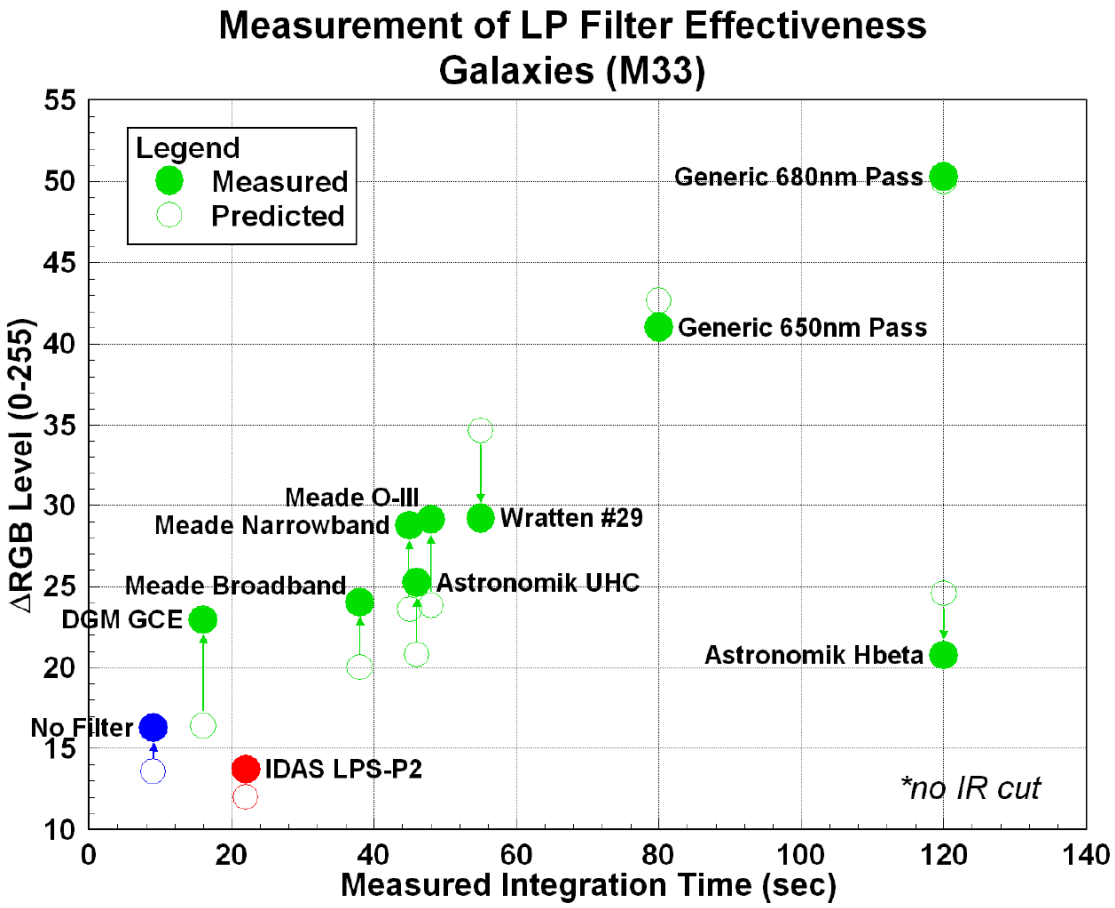

Figure 13 Measured LP Filter Effectiveness On Galaxies

The most interesting discovery for me was the performance of high pass filters, specifically reds and infrareds. In Figure 12 an outlier has been marked, the Lumicon Halpha Pass filter. This filter is essentially a dark red high pass filter. The performance of this filter on galaxies encouraged me to include colour filters in my analysis, including infrared high pass filters. The simplified plot of colour filter performance is shown in Figure 14. I have left out lines for colour groups that did not improve the ΔRGB by a significant amount. On bright nebulae there was some improvement realized from the blue and green filters, but not enough to make them competitive with traditional LP filters. On dim nebulae there is an improvement predicted using red and the shorter wavelength infrared pass filters, especially when combined with an IR cut filter. This is not surprising since this filter combo essentially makes a broad bandpass Halpha filter. The really interesting result was the performance of red and infrared filters on galaxies. Infrared pass filters are clearly superior to LP filters, with peak contrast occurring for an IR pass filter with a cut-off wavelength around 800nm. If you don't mind black-and-white images (you'll want to put your Saturation = 0) and the longer integration times, IR Pass filters may be the way to go on galaxies. Note that if you want to see Halpha regions in some of the closer galaxies, you'll have to select the appropriate high pass filter (ie. filter that does not cut off 656nm). The detailed plots for colour filters can be found in Appendix D.

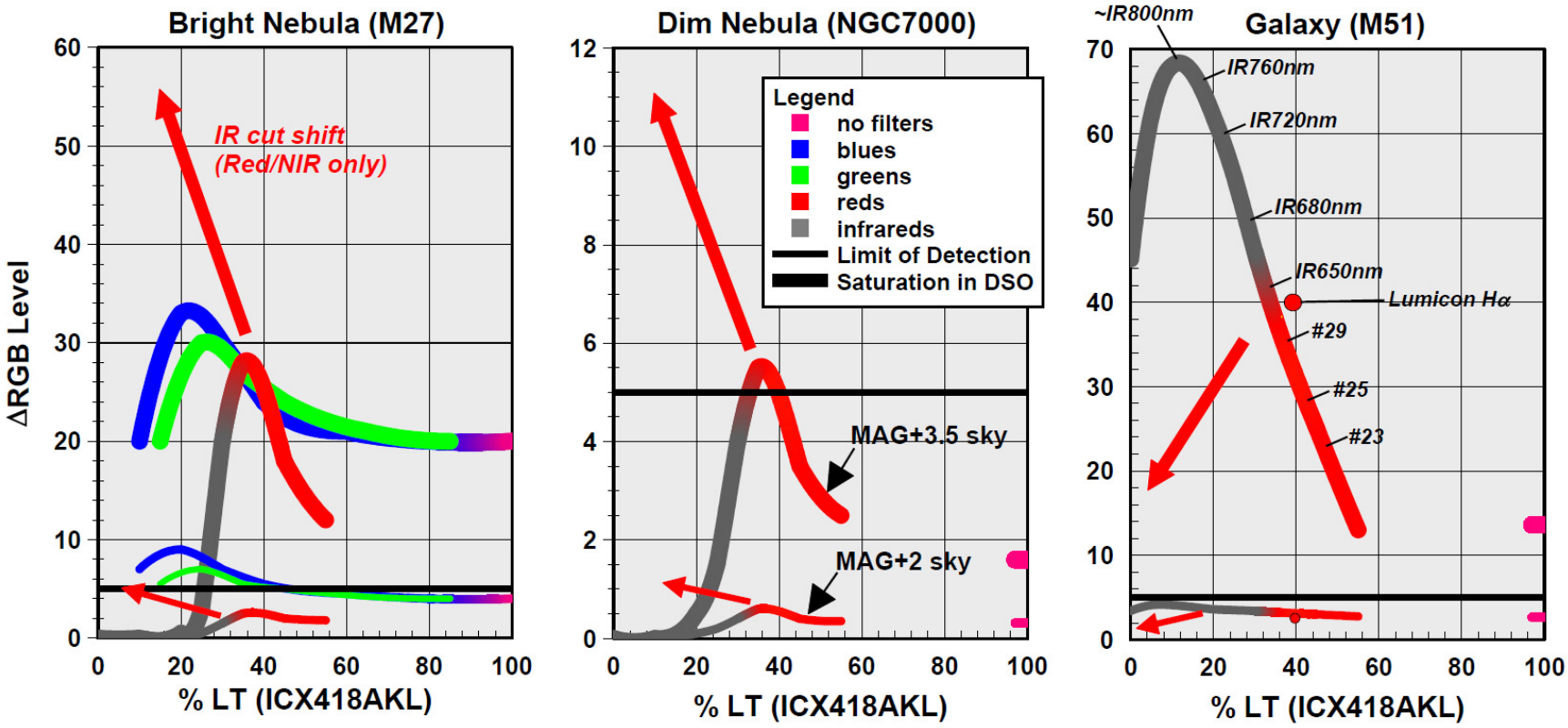

Figure 14 All Colour Filters - Simplified Video Performance Comparison

As with visual observing, the %LT of the filter you choose to use is important to how effective the filter is overall. The %LT has a direct impact on how long each video frame needs to be integrated for in order to get an image of reasonable brightness. A lower %LT means that less light is getting to the camera sensor, requiring longer exposures as a result. The camera I use, the Mallincam Xtreme, has a 99 minute limit on exposure time. However the exposure time that can actually be achieved depends heavily on how well your telescope is able to track the target. Thus in order to realize the benefits of using narrow filters like Halpha or IR Pass, you must be prepared to invest in a mount that can provide extended tracking, possibly through the use of guiding. In the many tests I have performed including the one mentioned above, I recorded the length of time required to achieve equivalent exposures for a selection of different filters. The resulting graph of integration time versus %LT is shown below.

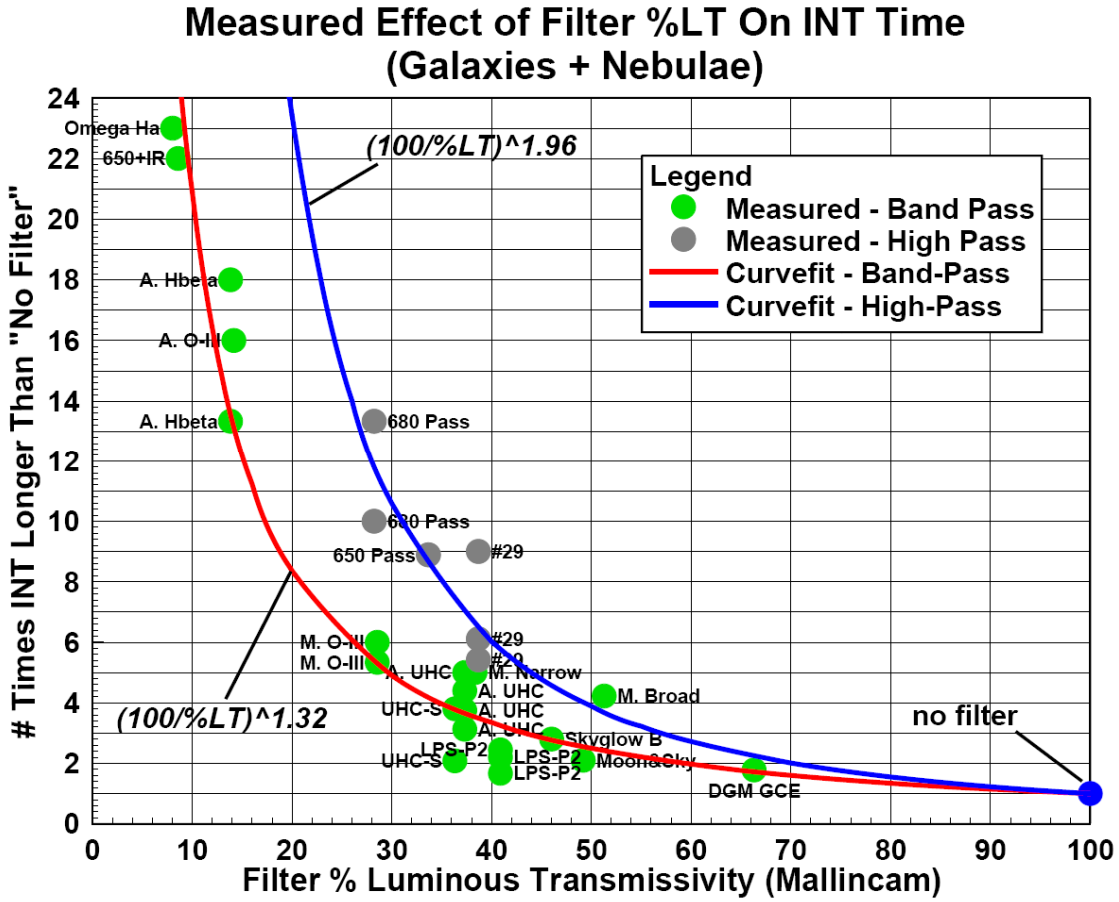

Figure 15 Measured Effect of %LT On Integration Time

I have applied a simple hyperbolic curvefit to the data, resulting in the following equations:

Band-Pass Filters: $(100 / \%LT)^{1.32}$

Red/IR High-Pass Filters: $(100/ \%LT)^{1.96}$

6.0 Filter Rating

I have found the results of my analysis to be very interesting and useful. The predicted performance for each filter in my database allows them to be compared equally and quantitatively, removing any uncertainty due to changing conditions or the subjectiveness of human observations. This could be useful information, but not in the form presented above and in the Appendices. Knowing the value of SNR or ΔRGB for a filter being considered for purchase does not necessarily make the decision of what to buy easier. I imagine that the question the consumer wants answered is:

"For my aperture of telescope, what is the best performing filter for me?"

The relationship between aperture and %LT was already established in Section 4 and 5 for visual and video observing respectively. The only part of the question remaining to be answered is "what is a good performing filter". To answer this I generated curvefits of all the SNR vs. %LT and ΔRGB vs. %LT data that represents a "nominal" filter performance. Excellent filters have performance above this nominal line, good filters are on the line, and bad filters have performance below this line. Figures 16 and 17 show the curvefits that were generated. The graphs are of base 10 log of filter efficiency versus %LT:

$$\text{Log}_{10}(\text{filter efficiency}) = \text{Log}_{10}[100*(\text{SNR}_{\text{with-filter}} - \text{SNR}_{\text{no-filter}})/\text{SNR}_{\text{no-filter}})/\%\text{LT}]$$

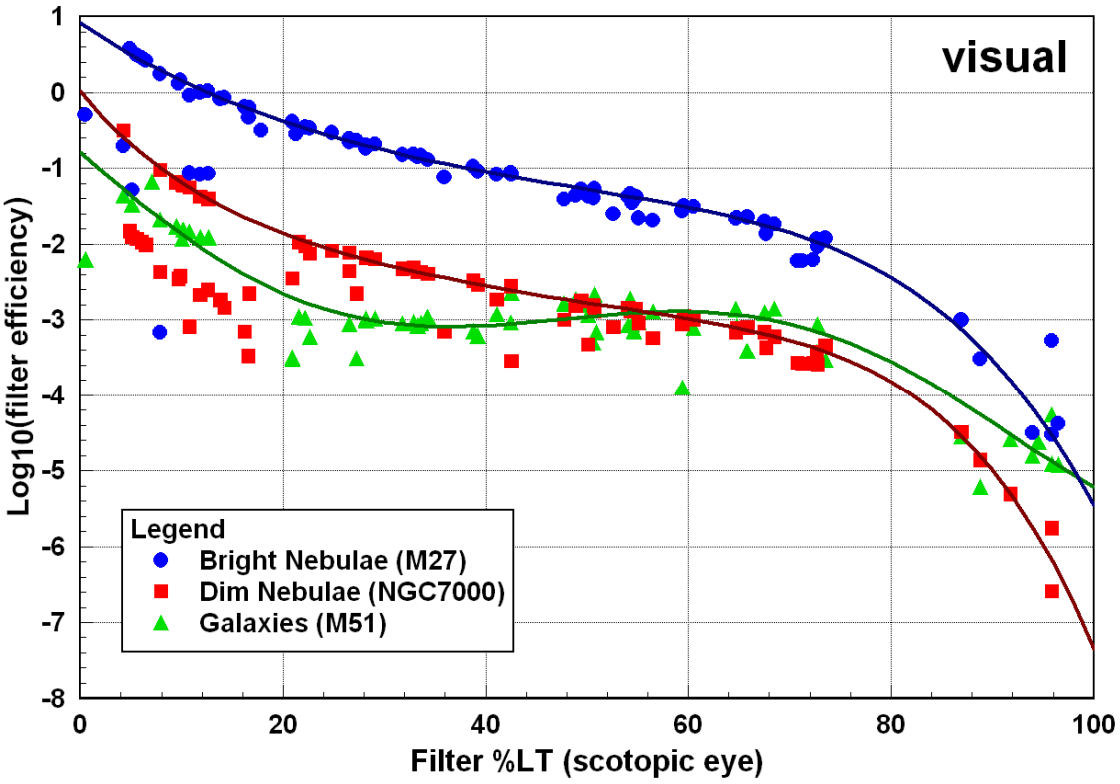

Figure 16 Filter Efficiency vs. %LT – Visual

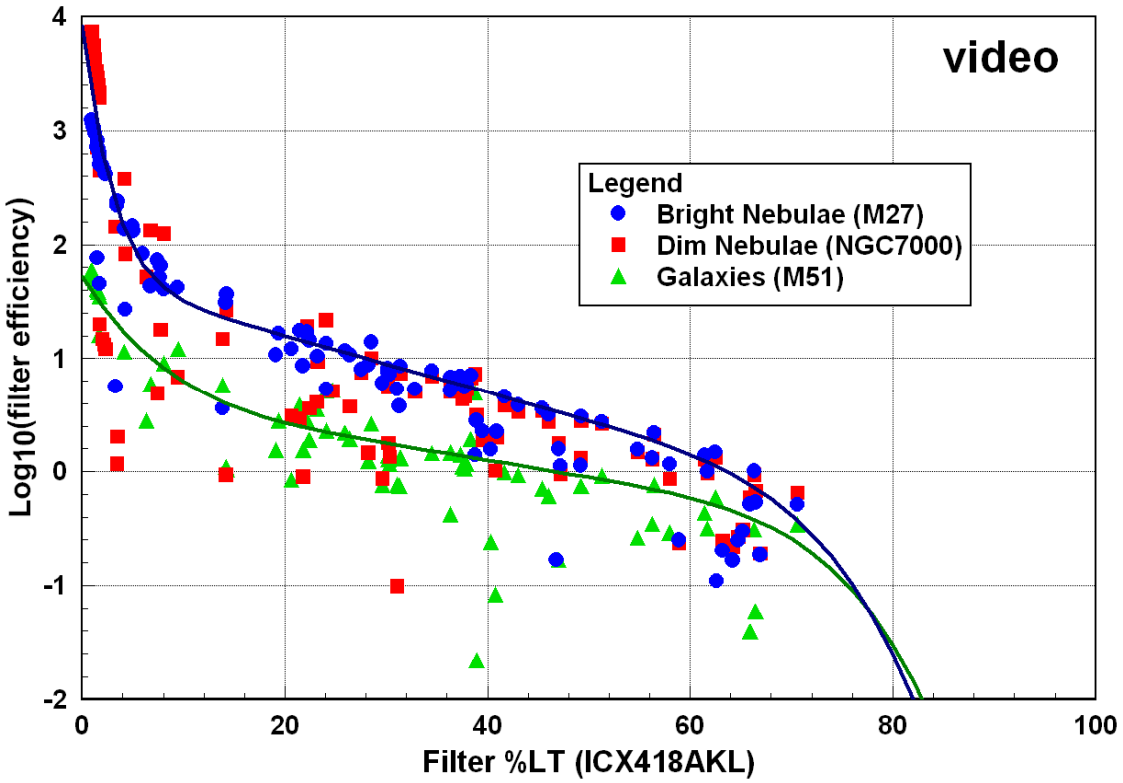

Figure 17 Filter Efficiency vs. %LT - Video

For the visual filter efficiency plots, the curvefits are all 5th order polynomials, but on the video filter efficiency plots they are 7th and 9th order. Also on the video filter efficiency plot, the data for bright and dim nebulae responses are on top of each other, and so they share a single curvefit. With these curvefits established, I was able to apply a grade to each filter based on their performance relative to the average for the corresponding %LT:

A+ filters >20% better than the average;

A filters 0-20% better than the average;

B filters 0-20% below the average;

C filters >20% below the average; and

D filters that are worse than no filter at all.

Tables summarizing the grading for every deep-sky filter in my database can be found in Appendix E. Filters are sorted in the tables by filter category and by %LT. From these tables I have generated short-lists of the best performing filters over the range of %LT. When combined with Figures 9 and 15, these short lists can be used to quickly select the best performing filter for a particular telescope setup. Note that in Table 4, the text is coloured to correspond with the monochrome colour of the filter. Filters providing full colour images are labeled in black.

LT Range	Filter	%LT	Grade		
			Bright Nebulae	Dim Nebulae	Galaxies
0-10%	Custom Scientific Hbeta	4.25	C	A+	B
	Custom Scientific O-III	4.85	A	C	D
	Baader Solar Continuum	7.04	D	D	A+
10-20%	1000 Oaks LP4	10.76	C	A	A+
	Lumicon O-III	12.57	A	C	D
	Astronomik Hbeta	12.63	C	A	A+
	Meade O-III	16.64	A	C	D
20-30%	Lumicon UHC	24.78	A	B	D
	1000 Oaks LP2	26.54	A	A	C
	Antares Narrow	29.06	A	A	A
30-40%	Andover 3ch Nebula	32.88	A	A	A
	Astronomik UHC	33.60	A	A	A
	Denkmeier UHC	38.76	A	A	B
40-50%	Televue Nebustar	42.49	A	A	A
	Astronomik UHC-E	42.52	A	C	A+
	Omega Wide	49.52	B	A	A+
50-60%	Arcturus Broad	50.74	A	B	A+
	Denkmeier Planetary	54.27	A	B	A+
	IDAS LPS-V3	54.84	A	A	B
	Antares ALP	59.58	A	A	B
60+%	Lumicon Deepsky	60.54	A	A	C
	Astronomik CLS	67.52	A	A	A
	Orion Skyglow Imaging	68.51	A	B	A+
	IDAS LPS-P1	73.54	A+	A+	C

Table 3 Top Performing Deep-Sky Filters - Visual Use

LT Range	Filter	%LT	Grade		
			Bright Nebulae	Dim Nebulae	Galaxies
0-2%	any Halpha <10nm wide	0.9 -	A+	A+	A*
2-5%	FLI O-III 8nm	2.13	A+	C	D
	Baader O-III	2.27	A+	C	D
	Orion Hbeta	3.28	C	A	D
	Astronomik Halpha 13nm	4.16	A+	A+	C*
5-10%	Baader Halpha 35nm	6.73	C	A+	C*
	Astronomik O-III CCD	7.42	A+	C	D
	Omega Halpha	8.04	C	A+	A*
	Baader Solar Continuum	9.45	D	D	A+*
10-20%	Astronomik Hbeta	13.84	C	C	A+*
	Astronomik O-III	14.17	A	C	C*
	IDAS O-III	14.23	A+	A	C*
20-30%	1000 Oaks LP3	21.43	A	C	A+
	Custom Scientific Multiband	22.17	A	A+	A
	1000 Oaks LP4	24.06	C	A+	A+
	Meade O-III	28.55	A+	A	A+
30-40%	Arcturus Narrow	36.34	A	A	A
	Astronomik UHC	37.32	A	A	A
	Meade Narrowband	38.34	A+	A+	A+
	Lumicon Halpha Pass	38.75	C	A+	A+
40-50%	Arcturus Broad	41.65	A	B	B
	1000 Oaks LP1	43.04	B	C	B
	Antares ALP	45.39	B	B	C
	Lumicon Deepsky	49.22	A	B	B
50-60%	Meade Wideband	51.3	A	A	A
	Astronomik CLS	56.45	A	A	A
60+%	Denkmeier Planetary	61.45	A	A	B
	Optec Deepsky	62.48	A+	A+	A
	DGM GCE	66.32	A+	A+	B
	Can-Tele Moon & Sky Glow	66.45	A	A	C

Table 4 Top Performing Deep-Sky Filters – Video Use

I do have a word of caution about the Meade brand filters listed in Table 4. My results are based on the manufacturer supplied spectral plots that came with my version of these filters. Historically Meade LP filters have varied widely in their performance due to quality control issues and changing filter suppliers over time. A good way to tell if you have a good performing version of a Meade filter is to hold it up to a bright light at arm's length and look through the filter. It should appear cyan, blue, or green depending on whether it is the Broadband, Narrowband, or O-III filter respectively. Now if you rotate the filter relative to your eye you should see the colour change. Your filter hopefully will change to magenta by the time you've rotated it by 30 to 45°, confirming that the filter is passing both O-III and H-alpha (which you want). If the filter changes colour to blue and not magenta when you rotate it, then the filter is not passing any H-alpha (which you don't want).

I also want to point out that although at %LT values below 20% the best filter for improving contrast in galaxies appears to be Halpha, my grading scheme hides the fact that in absolute terms the best contrast overall on galaxies is achieved by a filter in the 20 to 40% LT range. This does not include IR Pass filters, which I have found perform better than any deep-sky filter on galaxies.

7.0 Conclusions

The analysis method I have presented in this paper seems to be able to successfully predict the performance of different filters on different types of observed object. The actual performance values predicted for each filter may differ from reality somewhat, but the method appears to be sound and the results consistent with my personal observing experience.

Based on the results of my analysis, LP filters do actually work. Nothing can beat dark skies, but as long as one chooses the right filter for their telescope setup, significant improvements in your view can be achieved on nebulae under light polluted skies. Based on my analysis there is no significant improvement possible using a filter when viewing galaxies using an eyepiece. This finding changes if your detector is a CCD, where improvements can be achieved using a filter.

It is important to note that the results I've presented here are specific to the telescope configuration, DSO's, and LP levels that I've chosen. If I had chosen a telescope with a faster f/ratio or larger aperture, the predicted filter performance would be shifted upwards (ie. more observable). Similarly if the light pollution is milder or the DSO's had higher surface brightness, the absolute filter performance would also move up. My filter grades however should remain unchanged regardless of the telescope setup, the particular DSO, or the LP level.

I have used the results generated by my analysis method to assign a grade to every deep-sky filter I have in my database. Hopefully this grading system will be useful to other amateur astronomers as they search for affordable and effective light pollution filters.

For questions, contact me at: karmalimbo@yahoo.ca